

# Learning Cross-Modal Contrastive Features for Video Domain Adaptation

Donghyun Kim<sup>1</sup>, Yi-Hsuan Tsai<sup>2</sup>, Bingbing Zhuang<sup>2</sup>, Xiang Yu<sup>2</sup>  
 Stan Sclaroff<sup>1</sup>, Kate Saenko<sup>1,3</sup>, Manmohan Chandraker<sup>2</sup>

<sup>1</sup>Boston University, <sup>2</sup>NEC Labs America, <sup>3</sup>MIT-IBM Watson AI Lab

<sup>1</sup>{donhk, sclaroff, saenko}@bu.edu, <sup>2</sup>{ytsai, bzhuang, xiangyu, manu}@nec-labs.com

## Abstract

Learning transferable and domain adaptive feature representations from videos is important for video-relevant tasks such as action recognition. Existing video domain adaptation methods mainly rely on adversarial feature alignment, which has been derived from the RGB image space. However, video data is usually associated with multi-modal information, e.g., RGB and optical flow, and thus it remains a challenge to design a better method that considers the cross-modal inputs under the cross-domain adaptation setting. To this end, we propose a unified framework for video domain adaptation, which simultaneously regularizes cross-modal and cross-domain feature representations. Specifically, we treat each modality in a domain as a view and leverage the contrastive learning technique with properly designed sampling strategies. As a result, our objectives regularize feature spaces, which originally lack the connection across modalities or have less alignment across domains. We conduct experiments on domain adaptive action recognition benchmark datasets, i.e., UCF, HMDB, and EPIC-Kitchens, and demonstrate the effectiveness of our components against state-of-the-art algorithms.

## 1. Introduction

Recently, domain adaptation has gained a lot of attention due to its efficiency during training without the need of collecting ground truth labels in the target domain. Existing methods have made significant progress in image-based tasks, such as classification [33, 14, 54, 42], semantic segmentation [16, 53, 56, 31, 38] and object detection [8, 43, 24, 17]. While several works have sought to extend this success to video-based tasks like action recognition by aligning appearance (e.g., RGB) features through adversarial learning [6, 9, 37], challenges persist in video adaptation tasks due to the greater complexity of the video data. Moreover, different from the image data, domain shifts in videos for action recognition often involve more complicated environments, which increases the difficulty for adaptation. For

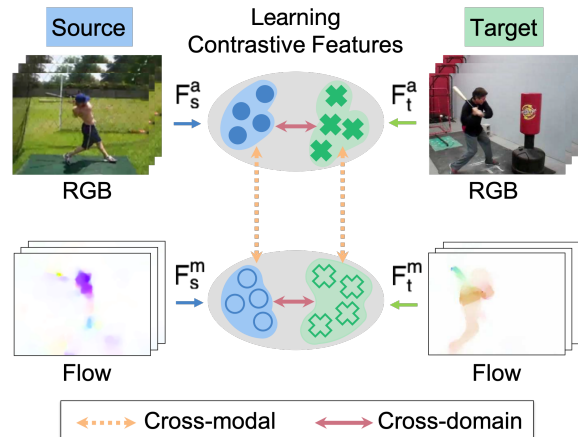


Figure 1. We propose a cross-modal contrastive learning framework for video domain adaptation. Our framework consists of two contrastive learning objectives: (1) cross-modal contrastive learning to align cross-modal representations from the same video, and (2) cross-domain contrastive learning to align representations between the source and target domains in each modality.

example, the “fencing” action usually happens in a stadium, but it can happen in other places such as home or outdoors. Also, different actions can take place under the same background. Therefore, purely relying on aligning RGB features can be biased to the background and affect the performance.

In addition to the appearance cue, other modalities such as motion, audio, and text are considered in (self-)supervised learning methods on the video data [46, 2, 26, 39]. In this work, we focus on appearance and motion as the two most common modalities in the cross-domain action recognition task, in which the motion modality (i.e., optical flow) is shown to be more domain-invariant (e.g., background changes) than RGB [36]. As a result, motion can better capture background-irrelevant information, while RGB can identify semantically meaningful information under different camera setups, e.g., camera perspective.

As shown in Figure 1, with two modalities across two domains, adaptation becomes a task of how to explore the relationship of cross-modal and cross-domain features, to fully exploit the multi-modal property for video domain

adaptation. That is, given either the source video  $V_s$  or the target one  $V_t$ , they can be associated to either the appearance feature  $F^a$  or the motion feature  $F^m$ , which results in four combinations of feature spaces, i.e.,  $F_s^a, F_t^a, F_s^m, F_t^m$ . Thus, the ensuing task is to design an effective adaptation mechanism for dealing with these four feature spaces. Since each modality has its characteristics and benefit (e.g., flow is more domain-invariant and RGB can capture semantic cues), it is of great interest to enable feature learning across the two modalities. Our key contribution stems from the observation that typical adversarial feature alignment schemes used in e.g. [6, 10] may not be directly applied in the cross-modal setting. For example, it is not reasonable to directly align the RGB feature  $F_s^a$  in the source domain with the flow feature  $F_s^m$  or  $F_t^m$  in either domain.

To tackle this issue, motivated by the recent advancements in self-supervised multi-view learning [50] that achieves powerful feature representations, we propose to treat each modality as a view, while introducing the cross-domain video data in our multi-modal learning framework. To this end, we leverage the contrastive learning objectives for performing feature regularization mutually among those four feature spaces (see Figure 1) under the video domain adaptation setting. We note that the prior work [36] also adopts a multi-modal framework, but it focuses on typical adversarial alignment and a self-supervised objective to predict whether the RGB/flow modality comes from the same video clip, without the exploration of jointly regularizing cross-modal and cross-domain features like our work.

More specifically, our framework is allowed to contrast features across modalities within a domain (e.g., between  $F_s^a$  and  $F_s^m$ ) or across domains using one modality (e.g., between  $F_s^a$  and  $F_t^a$ ). Two kinds of loss functions are designed accordingly: 1) a cross-modal loss that considers each modality as one view in a video while contrasting views in other videos from the same domain; 2) a cross-domain loss that considers one modality at a time and contrasts features based on the (pseudo) class labels of videos across two domains. There are several benefits of the proposed contrastive learning-based feature regularization strategies: 1) it is a unified framework that allows the interplay across features in different modalities and domains, while still enjoying the benefits of each modality; 2) it enables sampling strategies of selecting multiple positive and negative samples in the loss terms, coupled with memory banks to record large variations in video clips; 3) our cross-domain loss can be considered as a soft version of pseudo-label self-training with the awareness of class labels, which performs more robustly than typical adaptation methods.

We conduct experiments in video action recognition benchmark datasets, including the UCF [47]  $\leftrightarrow$  HMDB [27] setting, and the EPIC-Kitchens [11, 36] dataset. We show that including either our cross-modal or cross-domain con-

trastive learning objective improves accuracy while combining these two strategies in a unified framework obtains the best results. Moreover, our method performs favorably against state-of-the-art domain adaptation techniques, e.g., adversarial feature alignment [6, 36], self-learning scheme [10], and pseudo-label self-training. The main contributions of this work are summarized as follows.

- We propose a new multi-modal framework for video domain adaptation that leverages the property in four different feature spaces across modalities and domains.
- We leverage the contrastive learning technique with well-designed sampling strategies and demonstrate the application to adaptation for cross-domain action recognition by exploiting appearance and flow modalities.
- We show the effectiveness of both the cross-modal and cross-domain contrastive objectives, by achieving state-of-the-art results on UCF-HMDB and EPIC-Kitchens adaptation benchmarks with extensive analysis.

## 2. Related Work

In this section, we discuss existing fully-supervised and domain adaptation methods for action recognition, as well as methods on unsupervised learning for video representations.

**Supervised Action Recognition.** Action recognition is one of the important tasks for understanding video representations. With the recent advancements in deep learning, early works either adopt 2D [22] or 3D [19] convolutional networks on RGB video frames, which achieve significant progress. To improve upon the single-modal framework, optical flow is commonly used as the temporal cue to greatly improve the action recognition accuracy [46]. Following this multi-modal pipeline, several methods are proposed to further incorporate the long-term temporal context [58, 12] and structure [52, 66, 57], or extend to the 3D convolutional networks [4, 51]. Moreover, recent approaches show the benefit of adopting 1D/2D separable convolutional networks [52, 63], while other methods [12, 20] focus on improving the 3D convolutional architecture for action recognition, to be computationally efficient. Despite the promising performance of these methods in a fully-supervised manner, our focus is to develop an effective action recognition framework under the unsupervised domain adaptation setting.

**Domain Adaptation for Action Recognition.** Due to the convenience of recording videos under various conditions, there is an increasing demand for developing approaches for cross-domain action recognition. Previous methods focus on the setting of cross-domain transfer learning [49, 65, 64] or tackle the problem of view-point variance in videos [25, 29, 41, 45]. However, unsupervised domain adaptation (UDA) for action recognition has received less attention until

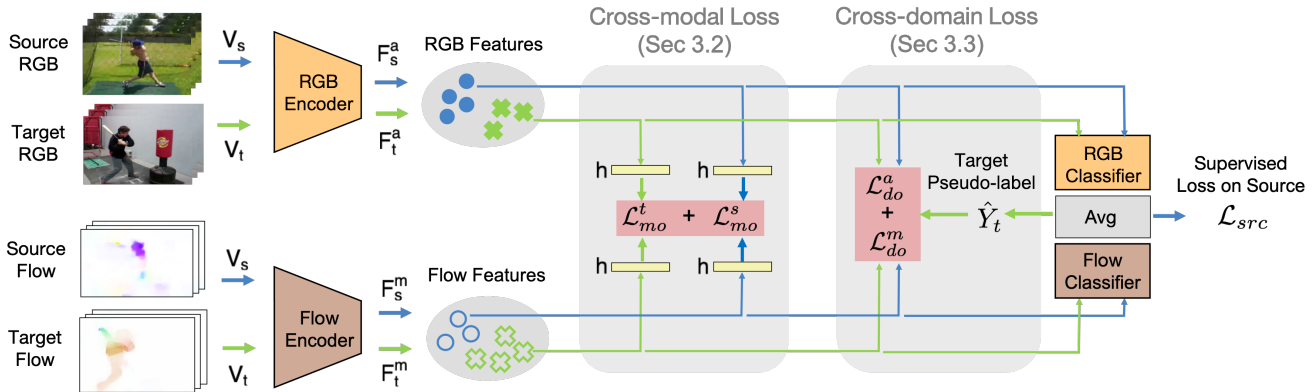


Figure 2. An overview of our cross-modal contrastive learning framework. We use a two-stream network for RGB and flow. Each stream takes video clips and outputs feature vectors for each domain and modality ( $F_s^a, F_t^a, F_s^m, F_t^m$ ). For cross-modal contrastive learning, we add the projection head ( $h$ ) to learn an embedding where the flow and RGB features from the same video are matched (e.g.,  $h(F_{s_i}^a), h(F_{s_i}^m)$ ). For cross-domain contrastive learning, we match the cross-domain features of the same class without the projection head (e.g.  $F_{s_i}^a, F_{t_j}^a$ ) in the same modality. For the unlabeled target domain, we use high-confidence pseudo-labels  $\hat{Y}_t$  to find positive samples in the source domain.

Table 1. Summary of notations.

Notation	Meaning
$\{V_s, V_t\}$	{Source, Target} video clips
$F_s^a$	Source appearance feature
$F_s^m$	Source motion feature
$F_t^a$	Target appearance feature
$F_t^m$	Target motion feature
$h(\cdot)$	Shared projection head
$\hat{Y}_t$	Target pseudo-label

recently. Early attempts align distributions across the source and target domains using hand-crafted features [3, 67], while recent deep learning based methods [18, 37, 9, 6, 10, 36] leverage the insight from UDA on image classification and extend it to the video case. For instance, approaches [6, 37] utilize adversarial feature alignment [14, 54] and propose a temporal version with attention modules. Moreover, self-supervised learning strategies are adopted by considering the video properties, such as clip orders [10], sequential domain prediction [5], and modality correspondence prediction [36] in videos. Similar to [36], our method also considers the multi-modal property, but focuses on a different problem regime. To be specific, we propose a contrastive learning framework that can better exploit the multi-modality to regularize the feature spaces simultaneously across modalities and across domains, which is previously unstudied.

### Self-supervised Learning for Video Representation.

Learning from unlabeled videos is beneficial for video representations as video labeling is expensive. For instance, numerous approaches are developed via exploiting the temporal structure in videos [13, 60], e.g., temporal order verification [34] and sorting sequences [28]. By leveraging the temporal connection across frames, patch tracking over time [59] or prediction of future frames [48] also facilitates feature learning in videos. Moreover, to incorporate the multi-modal information into learning, RGB frames, audio,

and optical flow are used to align with each other for self-learning [2, 26, 39, 15, 1, 35, 40]. After the learning process, such methods are usually served as a pre-training step for the downstream tasks. In this paper, we study the UDA setting for cross-domain and cross-modal action recognition, which involves a labeled source dataset and unlabeled target videos.

## 3. Proposed Method

In this section, we first introduce the overall pipeline of the proposed approach for video domain adaptation. Then we describe individual modules for cross-modal and cross-domain feature regularization, followed by the complete objective in a unified framework using contrastive learning.

### 3.1. Algorithm Overview

Given the source dataset that contains videos  $\{s_i\} \in V_s$  with its action label set  $Y_s$ , our goal is to learn an action recognition model that is able to perform reasonably well on the unlabeled target video set  $\{t_i\} \in V_t$ . Since we aim to investigate an effective way to construct a domain adaptive model that leverages the benefit of multi-modal information (i.e., RGB and flow) across domains, we utilize a two-stream network [36] that takes the RGB and flow images as the input. As a result, the two-stream network would output the RGB modality feature  $F^a$  and the flow modality feature  $F^m$ , which forms four different feature spaces across the modality and domain, i.e.,  $F_s^a, F_t^a, F_s^m, F_t^m$ .

In our contrastive learning framework, we jointly consider the relationship of these four spaces via two kinds of contrastive loss functions to regularize features as shown in Figure 1. First, we treat each modality as a view, extract the RGB/flow features from the same domain (either source or target), and contrast them based on whether the features come from the same video, e.g., the cross-modal features of one video,  $F_s^a$  and  $F_s^m$ , should be closer to each other in an embedding space than others extracted from different

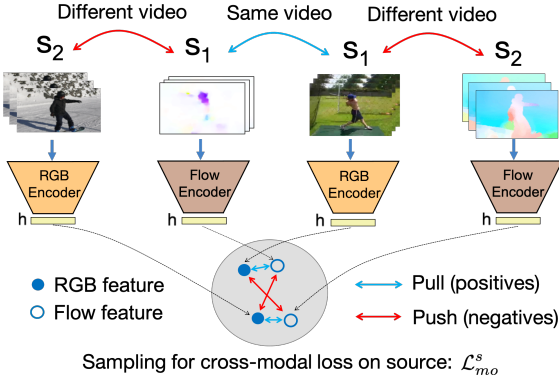


Figure 3. An overview of cross-modal contrastive learning. We pull an RGB feature and a flow feature from the same video clip as positives but push cross-modal features from different video clips.

video clips. Second, for features across the domains, e.g.,  $F_s^a$  and  $F_t^a$ , but within the same modality, we contrast them based on whether the videos are likely to share the same action label. To this end, we calculate the pseudo-labels  $\hat{Y}_t$  on target videos and form positive/negative samples to perform contrastive learning. Figure 2 illustrates our overall framework and Table 2 summarizes the notations.

### 3.2. Cross-modal Regularization

Motivated by the unsupervised multi-view feature learning method [50], we treat each modality as a view and form positive training samples within the same video, as well as negative samples from different videos. However, the difference is that we cannot directly apply negative pairing to all the videos, as in our problem, the videos from two different domains under the same view could still be largely different because of the domain gap. Therefore, it would not be proper to mix source and target videos, and instead, we form a contrastive objective in each domain separately.

**Sampling Strategy.** It has been studied that the sampling strategy is crucial in image-based contrastive learning [21]. Considering videos from one domain in our case, we select positive training samples from the same video but with different modalities, while sampling the negative ones when the RGB and flow frames are from different videos, regardless of their action labels. An illustration of cross-modal sampling for the source domain is in Figure 3, and a similar strategy is used for the target domain.

In addition, since one video clip contains many frames, every time we need to randomly sample a window of consecutive frames within a video clip, following the setting in [10, 36]. To account for the large intra-variation within a video clip, we do not assume that the RGB and flow modality need to have the same window of frames. For example, given a video clip, the RGB frames can be randomly sampled from the time window  $t \sim t + 15$ , while the flow frames can be different, e.g.,  $t + 5 \sim t + 20$ . Empirically, we find that

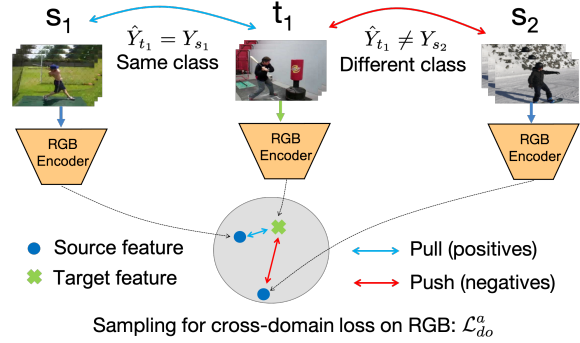


Figure 4. Based on pseudo-labels, we pull source and target features sharing the same labels but push cross-domain features otherwise.

such a sampling strategy is especially beneficial for our contrastive learning objective, which is aware of the variation within video clips in the embedding space.

**Similarity Between Samples.** Another important aspect in contrastive learning is the feature similarity. Taking the source domain as one example, we have features from RGB and flow, i.e.,  $F_s^a$  and  $F_s^m$ . Since each modality maintains its own feature characteristic, directly contrasting these two features may make the negative impact on the feature representation and reduce the recognition accuracy. To this end, given source features  $F_{s_i}$  and  $F_{s_j}$  from two videos  $\{s_i, s_j\} \in V_s$ , we apply an additional projection head  $h(\cdot)$  in a way similar to SimCLR [7], and then we can define the similarity function  $\phi^s(\cdot)$  between samples with a temperature parameter  $\tau$  as:

$$\phi^s(F_{s_i}^k, F_{s_j}^l)_{k,l \in \{a,m\}} = \exp(h(F_{s_i}^k)^\top h(F_{s_j}^l) / \tau). \quad (1)$$

where  $\{a, m\}$  represents either the appearance (RGB) or motion (flow) modality.

**Loss Function.** Based on the aforementioned sampling strategy and similarity measurement as depicted in Figure 3, the loss function for the source domain is written as:

$$\mathcal{L}_{mo}^s = -\log \frac{\sum_{s_i \in V_s} \phi^s(F_{s_i}^k, F_{s_{i+}}^l)_{k \neq l}}{\sum_{s_i \in V_s} \phi^s(F_{s_i}^k, F_{s_{i+}}^l)_{k \neq l} + \phi^s(F_{s_i}^k, F_{s_{j-}}^l)_{k \neq l}}, \quad (2)$$

where  $F_{s_{i+}}$  is the positive sample with a different view (modality) from the same video clip  $F_{s_i}$ , while  $F_{s_{j-}}$  is the negative sample with another view of a different video from  $F_{s_i}$ , regardless of their action labels. Here, we omit the notation  $k, l \in \{a, m\}$  to have a concise presentation.

On the other hand, for videos in the target domain, we construct another loss  $\mathcal{L}_{mo}^t$  similar to (2) with the same projection head  $h(\cdot)$ , where the similarity measurement  $\phi^t$  between features of target videos  $\{t_i, t_j\} \in V_t$  is defined as:

$$\phi^t(F_{t_i}^k, F_{t_j}^l)_{k,l \in \{a,m\}} = \exp(h(F_{t_i}^k)^\top h(F_{t_j}^l) / \tau). \quad (3)$$

Here, to consider individual domain characteristics, we find that the key is to form the cross-modal loss for each domain separately, while these two loss functions can still share the same projection head  $h^1$ . The projection head helps to prevent overfitting to this regularization. Without it, the RGB and flow features would be aligned to be the same, so that they are not complementary to each other anymore. Therefore, by combining these two loss functions in each of the source and target domains (i.e.,  $\mathcal{L}_{mo}^s$  and  $\mathcal{L}_{mo}^t$ ), features within the same video but from different modalities are closer in an embedding space, which is also served as a feature regularization on unlabeled target videos.

### 3.3. Cross-domain Regularization

In addition to the cross-modal regularization introduced in the previous section, we find that there is a missing connection between features across domains. To further exploit the interplay between four feature spaces ( $F_s^a, F_t^a, F_s^m, F_t^m$ ), we propose to use another contrastive learning objective for cross-domain samples.

**Sampling Strategy via Pseudo-labels.** Taking one modality, RGB, as the example, we consider cross-domain features of  $F_s^a$  and  $F_t^a$  in a similar contrastive learning setup as described in Section 3.2. Here, an intuitive way to form positive samples is to find the videos with the same label across domains. However, since we do not know the action label in the target domain, we first apply our two-stream action recognition model and obtain the prediction score of the target-domain video. Then, if the score is larger than a certain threshold  $T$  (e.g.,  $T = 0.8$  in our setting), we obtain the pseudo-label of this target sample and sample other source videos with the same action label from positive samples (otherwise they are negative samples). The procedure for the RGB modality is illustrated in Figure 4, while a similar way is used for the flow modality.

**Similarity Between Samples.** To measure the sample similarity in our contrastive objective, we adopt  $\phi^{st}$  to calculate the similarity between cross-domain features:

$$\phi^{st}(F_{t_i}^k, F_{s_i}^k)_{k \in \{a, m\}} = \exp(F_{t_i}^{k\top} F_{s_i}^k / \tau), \quad (4)$$

where the modality  $k$  can be appearance or motion in our work. Note that, for cross-domain feature regularization, in order to align features, we do not use an additional projection head  $h(\cdot)$  like Section 3.2 or Figure 3 (explained as the follows).

**Loss Function.** The corresponding loss function with respect to the sampling strategy (Figure 4) and the similarity

<sup>1</sup>We empirically find that using two individual projection heads for each domain produces a similar performance to the one that share the same projection head, so we use the shared projection head as a way for analyzing this embedding space later.

measurement  $\phi^{st}$  for the RGB modality is defined as:

$$\mathcal{L}_{do}^a = -\log \frac{\sum_{t_i \in \hat{V}_t} \phi^{st}(F_{t_i}^a, F_{s_{i+}}^a)}{\sum_{t_i \in \hat{V}_t} \phi^{st}(F_{t_i}^a, F_{s_{i+}}^a) + \phi^{st}(F_{t_i}^a, F_{s_{i-}}^a)}, \quad (5)$$

where  $t_i \in \hat{V}_t$  is the set of target videos with a more confident pseudo labels  $\hat{Y}_t$ .  $F_{s_{i+}}^a$  are the positive samples of source videos  $s_i \in V_s$  with the same class label as  $\hat{Y}_t$ , while  $F_{s_{i-}}^a$  are the negative samples with different class labels. Similarly, when the modality is flow, the loss function is:

$$\mathcal{L}_{do}^m = -\log \frac{\sum_{t_i \in \hat{V}_t} \phi^{st}(F_{t_i}^m, F_{s_{i+}}^m)}{\sum_{t_i \in \hat{V}_t} \phi^{st}(F_{t_i}^m, F_{s_{i+}}^m) + \phi^{st}(F_{t_i}^m, F_{s_{i-}}^m)}. \quad (6)$$

We also note that the choice without using the projection head  $h(\cdot)$  is reasonable as our objectives in (5) and (6) essentially try to make features with the same action labels closer to each other, which is consistent with the final goal for performing action recognition.

**Connections to Pseudo-label Self-training.** Using pseudo labels on the target sample to self-train the model is one commonly used approach in domain adaptation [69, 68, 32]. In the proposed cross-domain contrastive learning, we also adopt pseudo labels to form positive samples. However, these two methods are distinct, in terms of the way that reshapes the feature space.

Given the target video  $V_t$ , one can produce a pseudo-label  $\hat{Y}_t$  and use it for training the action recognition network with the standard cross-entropy loss. Therefore, such supervision is a strong signal that forces the feature  $F_t$  to map into the space of action label  $\hat{Y}_t$ , which is sensitive to noisy labels such as pseudo-labels. On the contrary, using contrastive learning with pseudo-labels is similar in spirit to the soft nearest-neighbor loss [44, 61], which encourages soft feature alignments, rather than enforcing the hard final classification, hence more robust to potential erroneous pseudo-labels. Similar observations are also presented in the recent work, which shows that the supervised contrastive loss [23] is more robust than the cross-entropy loss in image classification. In our case, we utilize such property and show that cross-domain contrastive learning can be achieved by using pseudo-labels in video domain adaptation, and is more robust than pseudo-label self-training. More empirical comparisons will follow in the experiments.

### 3.4. A Contrastive Learning Framework

In previous sections, we have introduced how we incorporate cross-modal and cross-domain contrastive loss functions to regularize features extracted from RGB/flow branches across the source and target domains. Next, we introduce the entire objective.

**Overall Objective.** Overall, we include loss functions in Section 3.2 and 3.3 without using any supervisions, and a standard supervised cross-entropy loss  $\mathcal{L}_{src}$  on source videos  $V_s$  with action labels  $Y_s$ . To obtain the final output from the two-stream network, we average the outputs from individual classifiers of RGB and flow branches (see Figure 2).

$$\mathcal{L}_{all} = \mathcal{L}_{src}(V_s, Y_s) + \lambda(\mathcal{L}_{mo}^s(V_s) + \mathcal{L}_{mo}^t(V_t) + \mathcal{L}_{do}(V_s, V_t, \hat{Y}_t)), \quad (7)$$

where  $\lambda$  is the weight to balance the terms. Here, we treat loss functions in (5) and (6) as one term:  $\mathcal{L}_{do} = \mathcal{L}_{do}^a + \mathcal{L}_{do}^m$ , as they are with the same form but using different modalities. Since all the loss terms are with a similar form, it does not require heavy tuning on each of them, so that we use the same  $\lambda$  for cross-modal and cross-domain losses (*i.e.*,  $\lambda = 1.25$  in this paper).

**Leveraging Memory Banks.** To compute the cross-modal and cross-domain loss functions, we need to compute all feature representations summed from video sets  $V_s$  and  $V_t$ . However, it is impossible to obtain all the features at every training iteration. Therefore, we store the features in the memory banks following [62], *i.e.*, an individual memory bank for a domain and a modality, totally with four combinations  $M_s^a, M_s^m, M_t^a$ , and  $M_t^m$ . Given the features in a batch (*i.e.*,  $F_{s_i}^a, F_{s_i}^m, F_{t_j}^a$ , and  $F_{t_j}^m$ ), we pull out features from the memory banks for positive and negative features (*e.g.*,  $F_{s_i+}^a$  or  $F_{s_i-}^a$  in (5) is replaced by  $M_{s_i+}^a$  and  $M_{s_i-}^a$ ). Then, the memory bank features are updated with the features in the batch at the end of each iteration. We use a momentum update  $\delta = 0.5$  following [62]:

$$M_{s_i}^a = \delta M_{s_i}^a + (1 - \delta) F_{s_i}^a. \quad (8)$$

The other memory banks,  $M_s^m, M_t^a$ , and  $M_t^m$ , are also updated in the same way. Using the momentum update also encourages smoothness in training dynamics [62]. In our case, during the training process, we randomly sample consecutive frames in a video clip. Therefore, by using the memory banks, our model can also encourage the temporal smoothness within each clip in feature learning.

## 4. Experimental Results

In this section, we show performance comparisons on numerous domain adaptation benchmark scenarios for action recognition, followed by comprehensive ablation studies to validate the effectiveness of our cross-domain and cross-modal feature regularization. Please refer to the supplementary material for more results and analysis.

### 4.1. Datasets and Experimental Setting

We use the three standard benchmark datasets for video domain adaptation, UCF [47], HMDB [27], and EPIC-Kitchens [11]. We then show that our method is a general

Table 2. Performance comparisons on UCF  $\leftrightarrow$  HMDB.

Setting	Two-stream	UCF $\rightarrow$ HMDB	HMDB $\rightarrow$ UCF
Source-only [6]		80.6	88.8
TA <sup>3</sup> N [6]		81.4	90.5
Supervised-target [6]		93.1	97.0
TCoN [37]		<b>87.2</b>	89.1
Source-only [10]		80.3	88.8
SAVA [10]		82.2	<b>91.2</b>
Supervised-target [10]		95.0	96.8
Source-only	✓	82.8	90.7
MM-SADA [36]	✓	84.2	91.1
Ours (cross-modal)	✓	<b>84.7</b>	92.5
Ours (cross-domain)	✓	83.6	91.1
Ours (final)	✓	<b>84.7</b>	<b>92.8</b>
Supervised-target	✓	98.8	95.0

framework to work for different types of action recognition settings: UCF  $\leftrightarrow$  HMDB for human activity recognition, as well as EPIC-Kitchens for fine-grained action recognition in egocentric videos.

**UCF  $\leftrightarrow$  HMDB.** Chen et al. [6] release the UCF  $\leftrightarrow$  HMDB dataset for studying video domain adaptation. This dataset has 3209 videos with 12 action classes. All the videos come from the original UCF [47] and HMDB [27] datasets, which sample the overlapping 12 classes out of 101/51 classes from UCF/HMDB, respectively. There are two settings of interest, UCF  $\rightarrow$  HMDB and HMDB  $\rightarrow$  UCF. We show the performance of our method in both settings following the official split provided by the authors [6].

**EPIC-Kitchens.** This dataset contains fine-grained action classes with videos recorded in different kitchens from the egocentric view. We follow the train/test split used in [36] for the domain adaptation task. There are 8 action categories in the three largest kitchens, *i.e.*, D1, D2, and D3, and we use all the pairs of them as source/target domains. Note that, compared to UCF  $\leftrightarrow$  HMDB, EPIC-Kitchens is more challenging as it has more fine-grained classes (*e.g.*, “Take”, “Put”, “Open”, “Close”) and imbalanced class distributions. We report the top-1 accuracy on the test set averaged over the last 9 epochs following [36].

**Implementation Details.** Our entire framework is implemented in PyTorch using 2 TITANXP GPUs. We use an I3D two-stream network [4] composed of an RGB stream and a flow stream, where the network is pre-trained on Kinetics following [10]. During training, we use the same setting as [10, 36] to randomly sample 16 consecutive frames out of a video clip. Then each RGB and flow stream takes these 16 frames with a size of  $224 \times 224$ . Each stream is followed by a fully-connected layer to compute individual output logits. Then the logits from each stream are averaged to predict the final class scores. To optimize the entire network, we use the SGD optimizer with a learning rate of 0.01. We set the temperature  $\tau = 0.1$  and  $\delta = 0.5$  for all experiments following [62]. For UCF  $\leftrightarrow$  HMDB, we follow the setting as [10] for batch size, total training epochs, learning rate, etc. For EPIC-Kitchens, we implement it upon the official code

Table 3. Performance comparisons on EPIC-Kitchens.

Setting	D2 → D1	D3 → D1	D1 → D2	D3 → D2	D1 → D3	D2 → D3	Mean	Gain
Source-only	42.5	44.3	42.0	56.3	41.2	46.5	45.5	
AdaBN [30]	44.6	47.8	47.0	54.7	40.3	48.8	47.2	+1.7
MMD [33]	43.1	48.3	46.6	55.2	39.2	48.5	46.8	+1.3
MCD [42]	42.1	47.9	46.5	52.7	43.5	51.0	47.3	+1.8
MM-SADA [36]	47.4	48.6	50.8	<b>56.9</b>	42.5	<b>53.3</b>	49.9	+4.4
Ours (modality)	44.3	50.2	49.5	56.6	43.0	48.8	48.7	+3.2
Ours (domain)	47.4	<b>52.8</b>	<b>52.4</b>	56.1	41.7	49.9	50.1	+4.6
Ours (final)	<b>49.5</b>	51.5	50.3	56.3	<b>46.3</b>	52.0	<b>51.0</b>	<b>+5.5</b>
Supervised-target	62.8	62.8	71.7	71.7	74.0	74.0	69.5	

of [36] but set the batch size as 32 to fit the memory of 2 GPUs and train the model for 6K iterations. The learning rate decreases by a factor of 10 every 3K iterations.

## 4.2. Results on UCF ↔ HMDB

We show experimental results for UCF → HMDB and HMDB → UCF in Table 2, comparing with state-of-the-art methods — TA<sup>3</sup>N [6], TCoN [37], SAVA [10], and MM-SADA [36].

**Comparisons with State-of-the-art Methods.** In each group of Table 2, in addition to the result for each method, we show the “Source-only” model that only trains on videos in the source domain, and the “Supervised-target” model that trains on target videos with ground truths, which serves as an upper bound. We also implement [36] on UCF-HMDB in the same setup for fair comparisons. Different from the TA<sup>3</sup>N, TCoN, and SAVA that only exploit the single modality via adversarial feature alignment and self-learning schemes, our method leverages both the RGB and flow modalities in a domain adaptation framework, which achieves the state-of-the-art performance. We also notice that our source-only model performs slightly better than the other source-only baselines, due to the usage of the flow stream. Despite that the domain gap is reduced by leveraging the flow modality, our approach still obtains comparable performance gains with respect to the source-only model and performs better than MM-SADA [36] that adopts the same two-stream model. For example, on UCF → HMDB, the gain for TA<sup>3</sup>N and SAVA is 0.8% and 1.9%, respectively, while our gain is the same as SAVA and is much higher than TA<sup>3</sup>N.

**Ablation Study.** In the fourth group of Table 2, we show model variants to validate the usefulness of individual components in our contrastive learning framework, *i.e.*, cross-modal and cross-domain feature regularization. From the results, the two modules consistently improve the performance over the source-only baseline. By combining both, it provides the highest accuracy. Here, interestingly, we find that the cross-domain module is less helpful than the cross-modal one. One reason is that on UCF ↔ HMDB, these two domains already share a high similarity, which reduces the impact of using the cross-domain loss. However, this

Table 4. Ablation study on EPIC-Kitchens.

Setting	Modality	Domain	Mean	Gain
Source-only			45.5	
MM-SADA [36]	✓		47.9	+2.4
Ours	✓		<b>48.7</b>	<b>+3.2</b>
MM-SADA [36]		✓	49.4	+3.9
Pseudo-labeling		✓	49.0	+3.5
Ours		✓	<b>50.1</b>	<b>+4.6</b>
MM-SADA [36]	✓	✓	49.9	+4.4
Ours	✓	✓	<b>51.0</b>	<b>+5.5</b>

also shows the importance of incorporating the proposed two modules, in which the cross-modal loss can still provide effective regularization, even when the domain gap is smaller. In the next section, we will show a different scenario, where both modules are important.

## 4.3. Results on EPIC-Kitchens

We present results on the EPIC-Kitchens benchmark for domain adaptation [36], including comparisons with state-of-the-art methods, ablation study, and more analysis.

**Comparisons with State-of-the-art Methods.** In Table 3, we present several domain adaptation methods, including distribution alignment via adversarial learning [33], maximum classifier discrepancy [42], and adaptive batch normalization [30], and a recently proposed method that uses a self-learning objective [36]. We note that these results are reported from [36] using the same two-stream feature extractor as ours, and they share the same “Source-only” model and “Supervised-target” upper bound in Table 3. For fair comparisons, we reproduce results of MM-SADA [36] using their official implementation and the same computing resources as ours, and show that our final model performs better than MM-SADA by 1.1% on average. The results show the advantages of our contrastive learning framework. More detailed analysis is provided as follows.

**Ablation Study.** In Table 4, we ablate the two components for our cross-modal and cross-domain loss functions with other approaches that consider the similar aspect. For fair comparisons, we use the same two-stream backbone, implementation, and computing resources for generating all the results. Considering only modality or domain, our method consistently performs better than MM-SADA [36], in which it uses a self-learning module to predict whether the RGB/flow modality comes from the same video clip and a typical adversarial learning scheme to align cross-domain features. Combining these two factors, our method improves the “Source-only” model the most, which shows the effectiveness of the proposed unified framework using contrastive learning. In addition, it is worth mentioning that our cross-domain loss performs better than pseudo-label self-training by 1.1%, which validates the discussion in Section 3.3 on

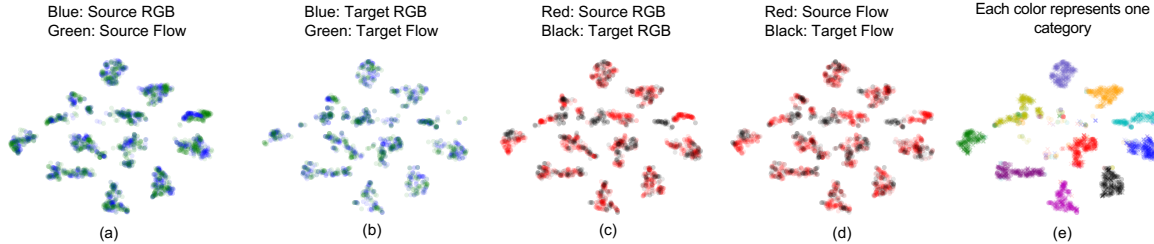


Figure 5. t-SNE visualization on cross-modal and cross-domain features after the projection head  $h(\cdot)$  on UCF  $\rightarrow$  HMDB, *i.e.*  $h(F_s^a)$ ,  $h(F_s^m)$ ,  $h(F_t^a)$ ,  $h(F_t^m)$ . In (a)(b), we show the visualization for individual domains, where each domain contains the multi-modality features. In (c)(d), we visualize features for each modality, and each plot uses the features from two domains. (e) includes all the features from two domains and two modalities, where each color represents one action class.

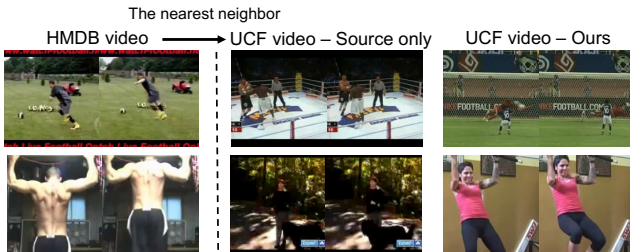


Figure 6. Cross-domain retrievals using the RGB feature. Given the target feature  $F_t^a$ , we retrieve the closest neighbor  $F_s^a$  in the source domain. Our model correctly aligns videos of the same class under view-angle (1st row) and background (2nd row) differences.

the difference of leveraging pseudo-labels.

**Sampling Strategy.** In Table 5, we present the ablation for sampling strategy in the cross-modal loss (see Section 3.2), where we do not assume that the RGB and flow modality have the same window of frames, which handles the large intra-variation within a video clip. When applying this strategy in MM-SADA [36], acting as a way for data augmentation, the performance gain is smaller than ours (*i.e.*, 0.5% vs 1.1%). This validates our sampling strategy with the proposed contrastive learning objective that enriches feature regularization under the domain adaptation setting.

#### 4.4. More Results and Analysis

We present more analysis including the feature visualizations using t-SNE [55], and example results for cross-domain retrieval to understand our model predictions.

**t-SNE Visualizations.** In this paper, we use a projection head  $h(\cdot)$  to project RGB/flow features to an embedding space for cross-modal loss in our framework. Therefore, it is of great interest to understand how the features behave in this embedding space. To this end, we sample features from both domains across two modalities, and perform t-SNE visualizations on UCF  $\rightarrow$  HMDB in Figure 5.

Here, although our cross-modal loss is calculated in each domain, the projection head is shared across the domains. Therefore, we provide different combinations of the feature spaces to visualize how the four feature spaces look like, *i.e.*,  $h(F_s^a)$ ,  $h(F_s^m)$ ,  $h(F_t^a)$ ,  $h(F_t^m)$ . First, in Figure 5(a)(b), it

Table 5. Ablation study on the sampling strategy.

Setting	Sampling	Mean	Gain via sampling
MM-SADA [36]		49.4	
	✓	49.9	+0.5
Ours		49.9	
	✓	51.0	+1.1

is not surprising to observe that in each domain, features from different modalities are aligned together (*e.g.*, Source RGB/Flow in Figure 5(a)), as it is exactly what the cross-modal objective in (2) optimizes for.

More interestingly, if we consider each modality at a time in Figure 5(c)(d), *e.g.*, Source RGB and Target RGB, their features are also aligned well, even we do not explicitly have an objective to align them in the embedding space via  $h(\cdot)$ . This shows the merit of our framework that enables feature regularization and interplay across four feature spaces. Also, we present a visualization on the distribution for each class, including all the source and target features across two modalities in Figure 5(e). This illustrates that features from the same category are aligned well.

**Cross-domain Retrievals.** In Figure 6, we show the cross-domain video retrievals using the RGB feature. Based on the target feature in HMDB, we show the nearest neighbor one from UCF. We show that our method can correctly retrieve the videos of the same class, either having the same context background but from a different view-angle or acting in a similar movement but with a different background.

## 5. Conclusions

We investigate the video domain adaptation task with our cross-modal contrastive learning framework. To this end, we leverage the multi-modal, RGB and flow information, and exploit their relationships. In order to handle feature spaces across modalities and domains, we propose two objectives to regularize such feature spaces, namely cross-modal and cross-domain contrastive losses, that learn better feature representations for domain adaptive action recognition. Moreover, our framework is modular, so it can be applicable to other domain adaptive multi-modal applications, which will be considered as the future work.

## References

- [1] Humam Alwassel, Dhruv Mahajan, Bruno Korbar, Lorenzo Torresani, Bernard Ghanem, and Du Tran. Self-supervised learning by cross-modal audio-video clustering. In *NeurIPS*, 2020. 3
- [2] Relja Arandjelovic and Andrew Zisserman. Look, listen and learn. In *ICCV*, 2017. 1, 3
- [3] Liangliang Cao, Zicheng Liu, and Thomas S Huang. Cross-dataset action detection. In *CVPR*, 2010. 3
- [4] J. Carreira and A. Zisserman. Quo vadis, action recognition? a new model and the kinetics dataset. In *CVPR*, 2017. 2, 6
- [5] M.H. Chen, B. Li, Y. Bao, G. AlRegib, and Z. Kira. Action segmentation with joint self-supervised temporal domain adaptation. In *CVPR*, 2020. 3
- [6] Min-Hung Chen, Zsolt Kira, Ghassan AlRegib, Jaekwon Yoo, Ruxin Chen, and Jian Zheng. Temporal attentive alignment for large-scale video domain adaptation. In *ICCV*, 2019. 1, 2, 3, 6, 7
- [7] Ting Chen, Simon Kornblith, Mohammad Norouzi, and Geofrey Hinton. A simple framework for contrastive learning of visual representations. In *ICML*, 2020. 4
- [8] Yuhua Chen, Wen Li, Christos Sakaridis, Dengxin Dai, and Luc Van Gool. Domain adaptive faster r-cnn for object detection in the wild. In *CVPR*, 2018. 1
- [9] Jinwoo Choi, Gaurav Sharma, Manmohan Chandraker, and Jia-Bin Huang. Unsupervised and semi-supervised domain adaptation for action recognition from drones. In *WACV*, 2020. 1, 3
- [10] Jinwoo Choi, Gaurav Sharma, Samuel Schulter, and Jia-Bin Huang. Shuffle and attend: Video domain adaptation. In *ECCV*, 2020. 2, 3, 4, 6, 7
- [11] Dima Damen, Hazel Doughty, Giovanni Maria Farinella, Sanja Fidler, Antonino Furnari, Evangelos Kazakos, Davide Moltisanti, Jonathan Munro, Toby Perrett, and Will Price. Scaling egocentric vision: The epic-kitchens dataset. In *ECCV*, 2018. 2, 6
- [12] C. Feichtenhofer, H. Fan, J. Malik, and K. He. Slowfast networks for video recognition. In *ICCV*, 2019. 2
- [13] Basura Fernando, Hakan Bilen, Efstratios Gavves, and Stephen Gould. Self-supervised video representation learning with odd-one-out networks. In *CVPR*, 2017. 3
- [14] Yaroslav Ganin, Evgeniya Ustinova, Hana Ajakan, Pascal Germain, Hugo Larochelle, François Laviolette, Mario Marchand, and Victor Lempitsky. Domain-adversarial training of neural networks. In *JMLR*, 2016. 1, 3
- [15] Tengda Han, Weidi Xie, and Andrew Zisserman. Self-supervised co-training for video representation learning. In *NeurIPS*, 2020. 3
- [16] Judy Hoffman, Eric Tzeng, Taesung Park, Jun-Yan Zhu, Phillip Isola, Kate Saenko, Alexei A. Efros, and Trevor Darrell. Cycada: Cycle-consistent adversarial domain adaptation. In *ICML*, 2018. 1
- [17] Cheng-Chun Hsu, Yi-Hsuan Tsai, Yen-Yu Lin, and Ming-Hsuan Yang. Every pixel matters: Center-aware feature alignment for domain adaptive object detector. In *ECCV*, 2020. 1
- [18] Arshad Jamal, Vinay P Namboodiri, Dipti Deodhare, and KS Venkatesh. Deep domain adaptation in action space. In *BMVC*, 2018. 3
- [19] S. Ji, W. Xu, M. Yang, and K. Yu. 3d convolutional neural networks for human action recognition. *IEEE Transactions on Pattern Analysis and Machine Intelligence*, 35(1):221–231, 2013. 2
- [20] Boyuan Jiang, MengMeng Wang, Weihao Gan, Wei Wu, and Junjie Yan. Stm: Spatiotemporal and motion encoding for action recognition. In *ICCV*, 2019. 2
- [21] Yannis Kalantidis, Mert Bulent Sariyildiz, Noe Pion, Philippe Weinzaepfel, and Diane Larlus. Hard negative mixing for contrastive learning. In *NeurIPS*, 2020. 4
- [22] Andrej Karpathy, George Toderici, Sanketh Shetty, Thomas Leung, Rahul Sukthankar, and Li Fei-Fei. Large-scale video classification with convolutional neural networks. In *CVPR*, 2014. 2
- [23] Prannay Khosla, Piotr Teterwak, Chen Wang, Aaron Sarna, Yonglong Tian, Phillip Isola, Aaron Maschiot, Ce Liu, and Dilip Krishnan. Supervised contrastive learning. In *NeurIPS*, 2020. 5
- [24] Taekyung Kim, Minki Jeong, Seunghyeon Kim, Seokeon Choi, and Changick Kim. Diversify and match: A domain adaptive representation learning paradigm for object detection. In *CVPR*, 2019. 1
- [25] Y. Kong, Z. Ding, J. Li, and Y. Fu. Deeply learned view-invariant features for cross-view action recognition. *IEEE Transactions on Image Processing*, 26(6):3028–3037, 2017. 2
- [26] Bruno Korbar, Du Tran, , and Lorenzo Torresani. Cooperative learning of audio and video models from self-supervised synchronization. In *NeurIPS*, 2018. 1, 3
- [27] H. Kuehne, H. Jhuang, E. Garrote, T. Poggio, and T. Serre. Hmdb: A large video database for human motion recognition. In *ICCV*, 2011. 2, 6
- [28] Hsin-Ying Lee, Jia-Bin Huang, Maneesh Singh, and Ming-Hsuan Yang. Unsupervised representation learning by sorting sequences. In *ICCV*, 2017. 3
- [29] Junnan Li, Yongkang Wong, Qi Zhao, and Mohan Kankanhalli. Unsupervised learning of view-invariant action representations. In *NeurIPS*, 2018. 2
- [30] Yanghao Li, Naiyan Wang, Jianping Shi, Xiaodi Hou, and Jiaying Liu. Adaptive batch normalization for practical domain adaptation. *Pattern Recognition*, 80:109 – 117, 2018. 7
- [31] Yunsheng Li, Lu Yuan, and Nuno Vasconcelos. Bidirectional learning for domain adaptation of semantic segmentation. In *CVPR*, 2019. 1
- [32] Qing Lian, Fengmao Lv, Lixin Duan, and Boqing Gong. Constructing self-motivated pyramid curriculums for cross-domain semantic segmentation: A non-adversarial approach. In *ICCV*, 2019. 5
- [33] Mingsheng Long, Yue Cao, Jianmin Wang, and Michael Jordan. Learning transferable features with deep adaptation networks. In *ICML*, 2015. 1, 7
- [34] Ishan Misra, C Lawrence Zitnick, and Martial Hebert. Shuffle and learn: unsupervised learning using temporal order verification. In *ECCV*, 2016. 3

- [35] Pedro Morgado, Yi Li, and Nuno Vasconcelos. Learning representations from audio-visual spatial alignment. In *NeurIPS*, 2020. 3
- [36] Jonathan Munro and Dima Damen. Multi-modal domain adaptation for fine-grained action recognition. In *CVPR*, 2020. 1, 2, 3, 4, 6, 7, 8, 11
- [37] Boxiao Pan, Zhangjie Cao, Ehsan Adeli, and Juan Carlos Niebles. Adversarial cross-domain action recognition with co-attention. In *AAAI*, 2020. 1, 3, 6, 7
- [38] Sujoy Paul, Yi-Hsuan Tsai, Samuel Schulter, Amit K. Roy-Chowdhury, and Manmohan Chandraker. Domain adaptive semantic segmentation using weak labels. In *ECCV*, 2020. 1
- [39] AJ Piergiovanni, Anelia Angelova, and Michael S. Ryoo. Evolving losses for unsupervised video representation learning. In *CVPR*, 2020. 1, 3
- [40] AJ Piergiovanni, Anelia Angelova, and Michael S Ryoo. Evolving losses for unsupervised video representation learning. In *Proceedings of the IEEE/CVF Conference on Computer Vision and Pattern Recognition*, pages 133–142, 2020. 3
- [41] Hossein Rahmani and Ajmal Mian. Learning a non-linear knowledge transfer model for cross-view action recognition. In *CVPR*, 2015. 2
- [42] Kuniaki Saito, Kohei Watanabe, Yoshitaka Ushiku, and Tatsuya Harada. Maximum classifier discrepancy for unsupervised domain adaptation. In *CVPR*, 2018. 1, 7
- [43] Kuniaki Saito, Yoshitaka Ushiku, Tatsuya Harada, and Kate Saenko. Strong-weak distribution alignment for adaptive object detection. In *CVPR*, 2019. 1
- [44] Ruslan Salakhutdinov and Geoff Hinton. Learning a nonlinear embedding by preserving class neighbourhood structure. volume 2 of *Proceedings of Machine Learning Research*, pages 412–419, 2007. 5
- [45] Gunnar A Sigurdsson, Abhinav Gupta, Cordelia Schmid, Ali Farhadi, and Karteek Alahari. Actor and observer: Joint modeling of first and third-person videos. In *CVPR*, 2018. 2
- [46] K. Simonyan and A Zisserman. Two-stream convolutional networks for action recognition in videos. In *NeurIPS*, 2014. 1, 2
- [47] Khurram Soomro, Amir Roshan Zamir, and Mubarak Shah. Ucf101: A dataset of 101 human actions classes from videos in the wild. *arXiv:1212.0402*, 2012. 2, 6
- [48] Nitish Srivastava, Elman Mansimov, and Ruslan Salakhutdinov. Unsupervised learning of video representations using lstms. In *ICML*, 2015. 3
- [49] Waqas Sultani and Imran Saleemi. Human action recognition across datasets by foreground-weighted histogram decomposition. In *CVPR*, 2014. 2
- [50] Yonglong Tian, Dilip Krishnan, and Phillip Isola. Contrastive multiview coding. In *ECCV*, 2020. 2, 4
- [51] D. Tran, L. Bourdev, R. Fergus, L. Torresani, and M. Paluri. Learning spatiotemporal features with 3d convolutional networks. In *ICCV*, 2015. 2
- [52] D. Tran, H. Wang, L. Torresani, J. Ray, Y. LeCun, and M. Paluri. A closer look at spatiotemporal convolutions for action recognition. In *CVPR*, 2017. 2
- [53] Yi-Hsuan Tsai, Kihyuk Sohn, Samuel Schulter, and Manmohan Chandraker. Domain adaptation for structured output via discriminative patch representations. In *ICCV*, 2019. 1
- [54] Eric Tzeng, Judy Hoffman, Kate Saenko, and Trevor Darrell. Adversarial discriminative domain adaptation. In *CVPR*, 2017. 1, 3
- [55] Laurens van der Maaten and Geoffrey Hinton. Visualizing high-dimensional data using t-sne. *Journal of Machine Learning Research*, 9:2579–2605, 2008. 8
- [56] Tuan-Hung Vu, Himalaya Jain, Maxime Bucher, Matthieu Cord, and Patrick Pérez. Advent: Adversarial entropy minimization for domain adaptation in semantic segmentation. In *CVPR*, 2019. 1
- [57] Limin Wang, Yuanjun Xiong, Zhe Wang, Yu Qiao, Dahua Lin, Xiaoou Tang, and Luc Van Gool. Temporal segment networks: Towards good practices for deep action recognition. In *ECCV*, 2016. 2
- [58] X. Wang, R. Girshick, A. Gupta, and K. He. Non-local neural networks. In *CVPR*, 2018. 2
- [59] Xiaolong Wang and Abhinav Gupta. Unsupervised learning of visual representations using videos. In *ICCV*, 2015. 3
- [60] Donglai Wei, Joseph Lim, Andrew Zisserman, and William T. Freeman. Learning and using the arrow of time. In *CVPR*, 2018. 3
- [61] Zhirong Wu, Alexei A Efros, and Stella Yu. Improving generalization via scalable neighborhood component analysis. In *ECCV*, 2018. 5
- [62] Zhirong Wu, Yuanjun Xiong, Stella X Yu, and Dahua Lin. Unsupervised feature learning via non-parametric instance discrimination. In *CVPR*, pages 3733–3742, 2018. 6
- [63] S. Xie, C. Sun, J. Huang, Z. Tu, and K. Murphy. Rethinking spatiotemporal feature learning for video understanding. In *ECCV*, 2018. 2
- [64] Tiantian Xu, Fan Zhu, Edward K. Wong, and Yi Fang. Dual many-to-one-encoder-based transfer learning for cross-dataset human action recognition. *Image and Vision Computing*, 55:127 – 137, 2016. 2
- [65] Xiao-Yu Zhang, Haichao Shi, Changsheng Li, Kai Zheng, Xiaobin Zhu, and Lixin Duan. Learning transferable self-attentive representations for action recognition in untrimmed videos with weak supervision. In *AAAI*, 2019. 2
- [66] Bolei Zhou, Alex Andonian, Aude Oliva, and Antonio Torralba. Temporal relational reasoning in videos. In *ECCV*, 2018. 2
- [67] Fan Zhu and Ling Shao. Enhancing action recognition by cross-domain dictionary learning. In *BMVC*, 2013. 3
- [68] Yang Zou, Zhiding Yu, B. V. K. Vijaya Kumar, and Jinsong Wang. Domain adaptation for semantic segmentation via class-balanced self-training. In *ECCV*, 2018. 5
- [69] Yang Zou, Zhiding Yu, Xiaofeng Liu, B.V.K. Vijaya Kumar, and Jinsong Wang. Confidence regularized self-training. In *ICCV*, 2019. 5

## Appendix

### A. Implementation Details

We use 2 TITANXP GPUs in our implementation. We also reproduce the results of MM-SADA [36]<sup>2</sup> using their released code with the same 2-GPU setup and the same batch size as our method.

### B. Ablation study

In Table 6, we show the sensitivity analysis on the  $\lambda$  (Eq. (7) in the main paper) and the confidence threshold  $T$  for pseudo-labels (Section 3.3 in the main paper).

In Table 7, we first show the benefit of having the projection head  $h(\cdot)$  for multi-modal embedding space. We observe a 2% performance gain by adding the projection head  $h(\cdot)$ , which demonstrates the importance of using  $h(\cdot)$  for multi-modal regularization described in Section 3.2 of the main paper. Moreover, we provide another ablation study where we add the projection head  $h(\cdot)$  in the cross-domain module, while having  $h(\cdot)$  for the cross-modal module as in our final model. Adding  $h(\cdot)$  shows slightly worse results than our final model. One reason is that this scheme has less influence on the features that are supposed to be aligned for performing action recognition.

In Table 8, we provide experimental results when different feature alignment methods are used in either cross-modal or cross-domain learning. In general, using the proposed contrastive learning method in both modules obtains the best performance, which shows the importance of having a unified contrastive learning framework for cross-modal and cross-domain learning.

Table 6. Ablation study on hyper-parameters on Epic-Kitchens. In the second group, we fix  $T = 0.8$ , while in the third group, we fix  $\lambda = 1.25$ .

Setting	Mean
Source-only	45.5
Ours ( $\lambda = 1.25, T = 0.8$ )	51.0
Ours ( $\lambda = 1.0$ )	50.1
Ours ( $\lambda = 1.5$ )	49.5
Ours ( $T = 0.9$ )	49.6
Ours ( $T = 0.6$ )	49.8

#### B.1. t-SNE Feature Visualizations

Figure 7 shows different combinations of the feature spaces before the projection head  $h(\cdot)$ , *i.e.*,  $F_s^a$ ,  $F_s^m$ ,  $F_t^a$ ,  $F_t^m$ . Figure 7-(a,b) shows the RGB and flow features in each domain. While the RGB and flow features are almost completely aligned after the projection head in Figure 3 of

<sup>2</sup><https://github.com/jonmun/MM-SADA-code>

Table 7. Ablation study on the projection head  $h(\cdot)$  for EPIC-Kitchens.

Setting	$h(\cdot)$ in cross-modal module	Mean
Ours (modality)	✓	48.7
Ours (modality)	✗	46.7
Setting	$h(\cdot)$ in cross-domain module	Mean
Ours (modality + domain)	✓	50.1
Ours-final (modality + domain)	✗	51.0

Table 8. Ablation study of different feature alignment methods on EPIC-Kitchens. “Con.” indicates our proposed contrastive learning approach, and “Adv.” denotes the adversarial learning scheme.

Setting	Modality	Domain	Mean
Con. (our final model)	Con.	Con.	51.0
Adv.	Adv.	Adv.	49.5
Adv. + Con.	Con.	Adv.	50.1

the main paper, here the RGB and flow features still keep their respective information before the projection head  $h(\cdot)$ , which is useful for final action predictions. Figures 7-(c,d) shows how the source and target features are aligned in each modality, where our method can learn domain-invariant features.

#### B.2. Visualizations for Cross-domain Retrievals

In Figure 8-(a), based on the target feature in HMDB, we show the nearest neighbor one from UCF. Similarly, we show the retrievals from EPIC Kitchens D1 and D2 in Figure 8-(b). EPIC-Kitchen is more challenging than UCF-HMDB as it has more common background (*e.g.*, similar kitchen backgrounds) or objects (*e.g.*, frying pan, utensils) between different action classes. Our method shows better results that retrieve the videos of the same class.

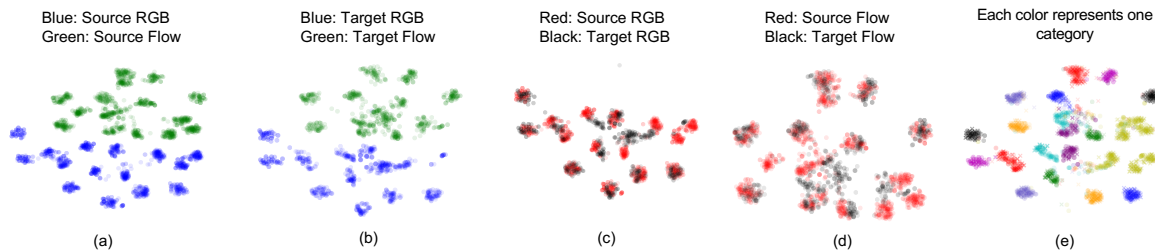
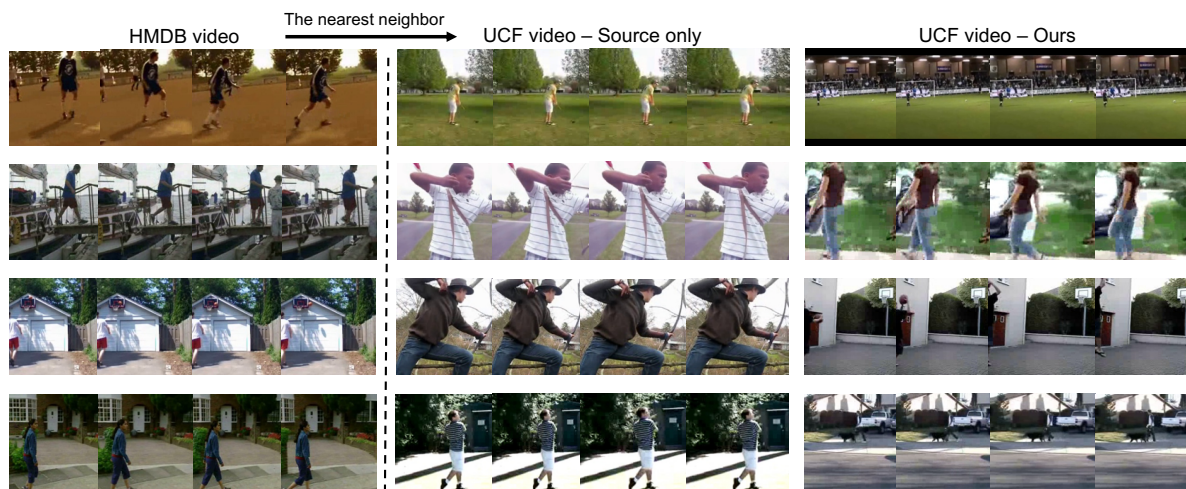
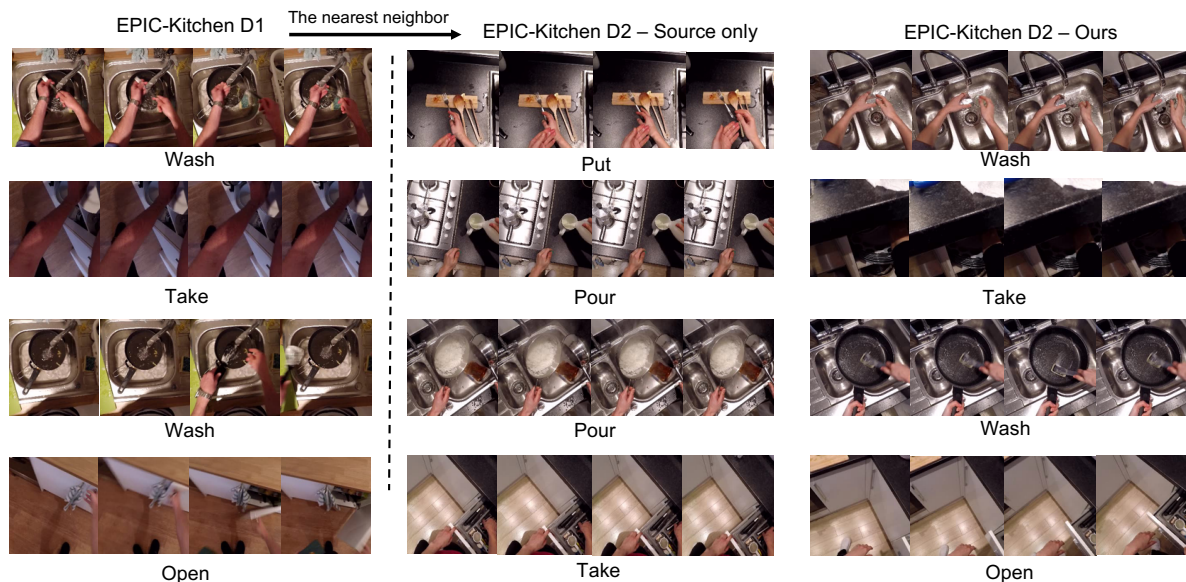


Figure 7. t-SNE visualization on cross-modal and cross-domain features before the projection head  $h(\cdot)$  on UCF  $\rightarrow$  HMDB, i.e.  $F_s^a, F_s^m, F_t^a, F_t^m$ . In (a)(b), we show the visualization for individual domains, where each domain contains the multi-modal features. In (c)(d), we visualize features for each modality, and each plot uses the features from two domains. (e) includes all the features from two domains and two modalities, where each color represents one action class.



(a) UCF  $\rightarrow$  HMDB



(b) EPIC-Kitchen D1  $\rightarrow$  D2

Figure 8. Cross-domain retrievals in the RGB embedding space. Given the target feature  $F_t^a$ , we retrieve the closest neighbor  $F_s^a$  in the source domain. By our contrastive learning framework, our model correctly aligns videos of the same class, while the source-only model are more likely to be biased to the background context.